ASPECTS OF RADIATION DAMAGE EFFECTS IN Fe-Cr ALLOYS FROM THE POINT OF VIEW OF ATOMISTIC MODELING

D. Terentyev

Institute of Nuclear Materials Science, SCK CEN, Boeretang 200, B2400, Mol.;

P. Olsson

Département Matériaux et Mécanique des Composants, EDF R&D, Les Renardières, F-77250 Moret-sur-Loing, France

E-mail: dterenty@sckcen.be

Fe-Cr alloys are the basis of high-Cr ferritic steels, which are the candidates for the structural materials for near future power plants. Recently, a significant effort has been put in the development of theoretical models dealing with the response of Fe-Cr alloys to irradiation. Here, we give a brief overview of the current level of understanding of radiation damage in Fe-Cr alloys, based on the most recent results. In particular, we review and summarize data obtained using different atomistic modelling techniques in order to refine the most important findings achieved over the past few years.

1. INTRODUCTION

High-Cr ferritic/martensitic steels are candidates for structural materials for a large number of future nuclear applications, from fusion to fission accelerator-driven systems and Gen IV reactors (e.g. [1] and references sited therein). Independently of the specific reactor concept, a reliable guide for the assessment of the behaviour of these steels in operation is the quantitative understanding of the basic physical mechanisms acting from the atomic to the macroscopic level and determining the response of the material to the applied mechanical, thermal and environmental loads, under neutron irradiation. The establishment of this knowledge is beneficial for the safe operation and design of most future nuclear installations. Fe-Cr alloys are the basis of high-Cr ferritic steels, so significant effort has been put, in the development of multi-scale models dealing with the response of Fe-Cr alloys to irradiation aimed at providing physical insight, rather than parameters of design interest. In this paper, we give a brief overview of the current level of understanding of radiation damage in Fe-Cr alloys, based on the most recent results obtained by different modelling techniques.

2. EXPERIMENTAL OBSERVATIONS SHOWING EFFECTS OF CR ON THE PROPERTIES OF IRRADIATED Fe-Cr ALLOYS

Experiments performed over the past thirty years clearly show that the addition of Cr to Fe influences significantly the response of the alloy to irradiation, non-monotonically with respect to the Cr content. One of the most pronounced effects of Cr is the suppression of void swelling, known since the late 1970 s [2]. This was explained by the trapping of point defects by Cr atoms, which consequently enhances the point defect recombination [2]. Another explanation proposed is the reduction of the dislocation network mobility due to the presence of <100> loops, whose population depends on C_{Cr} [3]. Indeed, the ratio ½<111>-to-<100> loops was found to increase with C_{Cr}, so that the microstructure of pure Fe and low Cr alloys is mainly composed of <100> loops [4]. In addition, in the alloys with Cr content large enough for the α-α' phase separation to occur, further reduction of swelling was observed, tentatively attributed to the role of Cr-rich precipitates acting as perfect sinks for point defects [5]. The mechanism of swelling reduction based on

ВОПРОСЫ АТОМНОЙ НАУКИ И ТЕХНИКИ. 2009. №4-1.
Серия: Физика радиационных повреждений и радиационное материаловедение (94), с. 68-79.

trapping of point defects imply that swelling should decrease with Cr content monotonically, whereas experimental measurements show a more complicated dependence. Swelling in neutron irradiated (up to dose ~30 dpa) Fe-Cr binary alloys is presented in Fig. 1,a. At 380 °C, swelling decreases with the addition of Cr and remains low for concentrations between 1 and 10% and then increases again in alloys with higher C_{Cr}. At higher temperatures (400-460 °C), the minimum of swelling shifts towards lower C_{Cr} and is located around 3...6% Cr. But at the same time, swelling is also reduced in alloys containing more than 10% Cr, resulting in a local maximum at ~10% Cr. Further increase of temperature up to 615 °C leads to the restoration of the minimum around 10%.

A remarkable effect of Cr is also seen in the reduction of the shift in the ductile-to-brittle transition temperature (ΔDBTT) in both high-Cr steels and binary alloys. ΔDBTT was found to reach a minimum around 9% Cr [6], in a range of irradiation temperatures 300…410 °C and doses 7-36 dpa. Recent experiments on Fe-Cr binary alloys, irradiated in the BR2 reactor at 300 °C up to 1.5 dpa, also demonstrate that radiation-induced hardening ($\Delta\sigma_y$), shown in Fig.1,b, is higher in Fe-Cr alloys and saturates at higher dose, than in pure Fe [7]. Again, the dependence of $\Delta\sigma_y$ on C_{Cr} is not regular: it is larger than in Fe, remains almost independent of Cr content with a minimum at ~9% Cr, and then increases again [7]. The increase of $\Delta\sigma_y$ above 9% Cr is qualitatively understandable in terms of α-α' phase separation [8], however, no explanation why there is an increase of the ΔDBTT and $\Delta\sigma_y$ below 9% Cr so far exists. Both swelling and hardening are closely related with the microstructure formed during irradiation. In the case of moderate doses (i.e. few dpa, so relevant for $\Delta\sigma_Y$ shown in Fig.1,c), the main defects detected using transmission electron microscopy (TEM) are interstitial dislocation loops. Experiments clearly show that the presence of even small percentages (0.1%) of Cr in ultra-pure Fe enhances the nucleation of interstitial type dislocation loops, with a subsequently higher radiation-induced hardening [9]. Enhancement of ½<111> loop density in Fe10%Cr irradiated by electrons at 25 °C has been also reported [10]. Finally, *in-situ* TEM studies show higher thermal stability of ½<111> loops in ultra pure Fe9%Cr than in Fe [11]. The density of <100> loops formed after severe neutron irradiation also depends on C_{Cr} as shown in Fig.1,c [5].

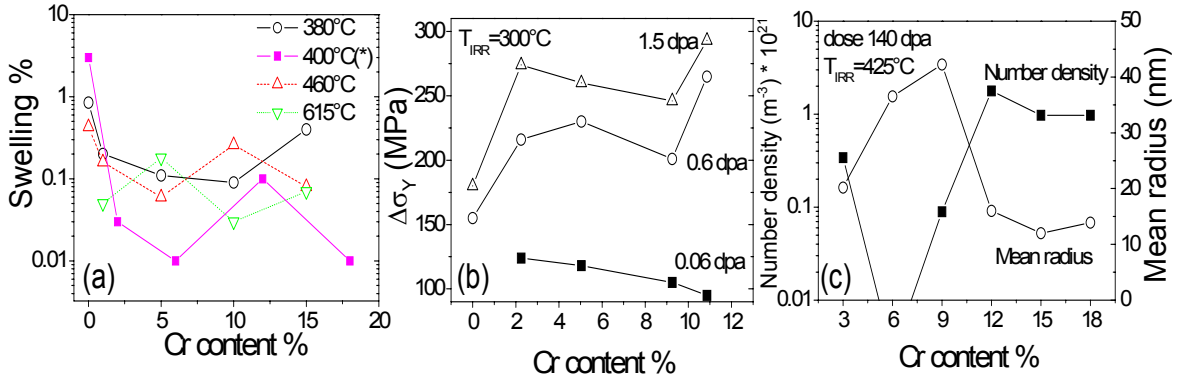

Fig. 1. Swelling in the Fe-Cr alloys irradiated up to 30 dpa in the DFR fast reactor [2], (*) refers to the alloys irradiated in BR-10 fast reactor up to 26 dpa [12] (a). Change in the yield stress in the alloys irradiated in BR-2 at 300 °C up to dose 0.06-1.6 dpa [7] (b). Density and mean size of <100> dislocation loops observed in the alloys irradiated in FFTF/MOTA at 425 °C up to 140 dpa [5] (c)

Understanding of such an interplay of the radiation-induced swelling, hardening, embrittlement and microstructure features significantly varying with Cr content is required. The role of atomistic modelling is to envisage mechanisms involved in radiation phenomenon which otherwise can not be rationalized directly (or even indirectly) from experiments. These are, for example, primary damage, migration of point defects and their

nano-clusters, interaction of dislocations with dislocation loops, etc. In other words, processes occurring at the space and time scale inaccessible on the experimental level. Here, we summarize recent findings achieved using different modelling techniques and discuss implications of these findings.

3. RECENT PROGRESS IN ATOMISTIC SIMULATIONS

3.1. Mixing enthalpy of Fe-Cr alloys

Experimental measurements of short range order (SRO) parameter, performed after thermal ageing and under irradiation [13], revealed that it changes sign from negative to positive at ~10% Cr. This implies that Cr atoms repel each other in the alloys with C_{Cr}<10%, thus providing a large solubility limit, and tend to segregate only if C_{Cr} exceeds ~10%. The physical origin of this phenomenon was recently explained based on results from density functional theory (DFT) calculations, showed that the mixing enthalpy (ME) of random Fe-Cr alloys also changes sign from negative to positive at ~8% Cr, with a minimum around 5% Cr [14]. The origin of the negative ME and repulsion between Cr atoms is a two fold band structure effect [35] and the so-called 'magnetic frustration' effect [15]. The former explains the fact that the substitution of Cr in Fe has a negative heat of mixing by the effective lowering of the occupation at the Fermi level as Cr is introduced. The latter is because each Cr atom favours its magnetic moment antiparallel to the host Fe atoms as well as to Cr first nearest neighbours. In dilute alloys, the most energetically favourable situation is obtained when the Cr atoms are distributed sufficiently far from each other to avoid magnetic frustration, which induces SRO and even probably long range order in the alloys containing 6.25 and 3.7 % Cr as proposed in [16, 17]. By increasing Cr concentration, Cr-Cr interactions cannot be avoided anymore and this leads to a positive heat of mixing, resulting in the Cr precipitation or α-α' phase separation.

Based on the data obtained with DFT, for the first time, the central-force many body potential allowing to reproduce correct heat of mixing of Fe-Cr system was developed [18]. The cross-potential describing Fe-Cr interaction allows for the effect of not only *d*-band, as standard EAM potential does, but also *s*-band electrons, thus successfully reproducing the heat of mixing from DFT [18]. The potential therefore was called the 'two-band' model, so we will refer to as the 2BM potential. The Fe-Fe part of the potential is from [19], which is a significant improvement over previous models (see [19] for details) from the point of view of properties of self-interstitial atoms (SIA) and their small clusters as compared to DFT [20].

3.2. Primary damage in Fe-Cr alloys and pure Fe

A complete comparative study of displacement cascades in random Fe-Cr alloys (with C_{Cr}=5,10 and 15%) and pure Fe simulated with 2BM potential can be found in [21]. It has been shown that no significant difference in the primary damage state between Fe and Fe-Cr alloys exists in terms of number of defects produced, clustered fractions and cluster size distributions. In Fe-5%Cr and Fe-10%Cr alloys, SIAs and SIA-clusters were found to be bound to Cr atoms. Most of single SIAs appear as mixed <110> dumbbells. Small <110> SIA clusters, containing up to 5 defects, were not 'enriched' by Cr. Concentration of Cr inside larger <111> SIA clusters, is greater by about 3 and 1.5 times than in Fe-5%Cr and Fe-10%Cr matrices, respectively. Enrichment of SIA defects by Cr was not detected in Fe-15%Cr. Formation of Cr-Cr dumbbells was almost never observed in all studied alloys. A very small but statistically meaningful change of the SRO parameter in Fe-5%Cr and Fe-15%Cr was detected, whereas no change occurred in Fe-10%Cr. The change to negative SRO parameter in Fe-5%Cr was due to the break-up of the Cr-Cr first nearest neighbour (1st nn) pairs, while changes to positive SRO parameter in Fe-15%Cr was due to the formation of Cr clusters during solidification of the molten region.

The details of the different arrangements of Cr atoms near interstitial defects are, however, of minor importance for the post-cascade long-term evolution. The main message received from the comparative study of cascades in Fe and Fe-Cr alloys is that the number density

and size distribution of defects produced are not affected by the presence of Cr. Observation of the cascade-induced Cr ordering and clustering is potentially important but it is not clear for the moment if this effect could be as effective as phase changes driven by cascade-induced defects.

3.3. Mobility of point defects and their clusters in Fe and Fe-Cr alloys

The mobility of point defects and their clusters is one of the most important parameters determining the microstructure evolution in irradiated metals. Thus, the precise knowledge of migration properties of vacancy and interstitial defects versus defect size is a fundamental prerequisite for any model intended to describe microstructure evolution under irradiation. One of the conventional ways to study migration properties of elementary point defects and their small clusters in metals is to perform measurements of resistivity by during isochronal annealing of pre-irradiated samples. Resistivity recovery studies performed in dilute and concentrated alloys (up to 15% Cr) have shown that the recovery indeed depends on the Cr content (for review and most recent result see [22]). The recovery stages associated with the onset of a single SIA and Di-SIA cluster (in pure Fe) were found to be significantly affected by Cr in concentrated alloys. Whereas, the stage attributed to the vacancy long-range migration remains unchanged. This was interpreted in terms of no influence of Cr atoms on the vacancy migration. Similar conclusion was drawn based also on results of positron annihilation spectroscopy. At the same time, DFT studies have also shown that the interaction of Cr atoms with a single vacancy in Fe is negligibly small (for review and the most recent results see [23]). Comparative MD study of vacancy migration in pure Fe and Fe-12%Cr have shown that the difference between migration energy estimated in pure metal and in the alloys is only 0.07 eV (lower in alloy) [24]. We therefore focus on the study of the mobility of SIA defects, since these are mainly seen to be affected by Cr in experiments.

3.3.1. Classification of SIA clusters

Prior to considering the effect of Cr on the mobility of SIA defects, it is useful to give a brief overview of the recent DFT and MD findings with respect to the properties of SIA defects in pure Fe. DFT studies suggest that a single SIA and SIA clusters with size up to five defects occupy a <110> configuration (preferred to <111>) and therefore while migrating follow a 3D path by performing translation-rotation jumps via movement of individual <110> dumbbells [20, 25]. The ground state for larger SIA clusters is a platelet of <111> crowdions which consequently exhibit 1D-motion [26]. Using accurate DFT calculations, the migration energy of a single SIA was found to be 0.33 eV, and this was also well reproduced by the 2BM potential [27]. The migration energies of 3D moving SIA clusters were estimated to vary from 0.15 up to 0.4 eV using both static DFT calculations [20] and MD simulations with the 2BM potential [25]. MD study of the mobility of <111> SIA clusters with the 2BM potential has shown that the migration energy weakly depends on the cluster size and it was estimated to be ~0.05 eV [25]. It is therefore important to keep in mind that even relatively large (up to few tens of defects) <111> SIA clusters exhibit fast 1D motion in contrast to small 3D-migrating SIA clusters.

3.3.2. Interaction of SIA with Cr atoms in dilute solution

A thorough study of the interaction of a single SIA and Cr atoms by DFT and with the 2BM potential in pure Fe was performed in [23, 27]. It has been found that single SIAs interact strongly and mainly attractively with Cr atoms. The strength and sign of the interaction depends on the local Cr distribution, as well as on the configuration of the SIA, which could be a <110> dumbbell or <111> crowdion, as shown in Fig.2. A dumbbell is bound to an isolated Cr atom therefore forming a mixed (i.e. Fe-Cr) dumbbell and the energy required to separate a Cr and dumbbell is about 0.1 eV (Fig.2, #1). The presence of a second Cr nearby an Fe-Cr dumbbell may increase the binding energy up

to 0.15 eV (Fig.2, #2) or results in a repulsive interaction (Fig.2, #5), depending on the particular arrangement of Cr atoms. The highest repulsion (0.42 eV) occurs when the two Cr atoms form a dumbbell (Fig.2, #5). This repulsion stems from the effect of magnetic frustration determining Cr-Cr repulsion in Fe. The binding energy of a <111> crowdion to an isolated Cr (Fig.2, #4) was found to be much higher than that with a dumbbell. However, the formation energy of an Fe-Cr crowdion is still higher than that of an Fe-Cr dumbbell (the excess formation energy is 0.4 eV), so the most stable configuration of an SIA is the mixed dumbbell [23, 27].

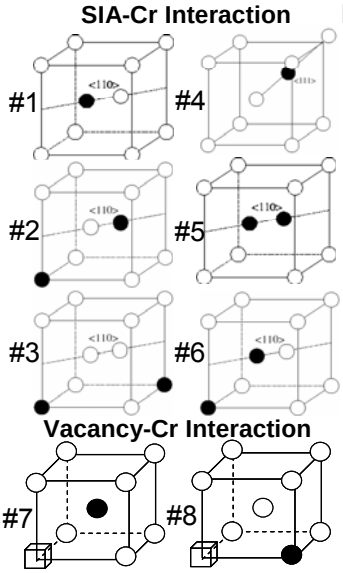

Interaction energy (eV)

	DFT	Potential
Interstitial – Cr		
#1	-0.08	-0.14
#2	-0.15	-0.05
#3	-0.15	-0.19
#4	-0.37	-0.4
#5	0.42	0.33
#6	0.21	0.1
Vacancy – Cr		
#7	0.057	0.007
#8	0.014	-0.0053

Fig. 2. Interaction between Cr atoms and point defects [27]. Filled circle denotes a Cr atom, empty cube denotes a vacancy

The mobility of a single SIA in random Fe-Cr alloys (with C_{Cr}=1-15%) was studied by MD simulations [27]. The results obtained have shown that an SIA migrates via translation-rotation jumps as in pure Fe and this mechanism is shown in Fig.3,a. The SIA migration energy, E_m(SIA), estimated from the Arrhenius slope was seen to slightly decrease with Cr content (e.g. in Fe-15%Cr was reduced by 0.1 eV), as compared to the pure Fe, where E_m(SIA)=0.31 eV. As a consequence of this, at low temperature the SIA appears to migrate faster in Fe-Cr alloys. At the same time, a reduction of the SIA diffusivity at high temperature was expressed in the prefactor, found to decrease monotonically with Cr content. The migration of the SIA in concentrated alloys was found to be irregular i.e. the time delay before a jump differed significantly, sometimes reaching few nano-seconds in simulations performed at 300 °C. This was explained by the presence of some low energy states for the SIA, producing a trapping effect [27]. The migration of the SIA in the alloys with C_{Cr} not exceeding 10% preferentially occurred via movement of the mixed dumbbell, thus mainly contributing to the Cr mass transport. The preferential motion of the mixed dumbbell is not only determined by the binding energy, but also due to the lower migration barrier, as can be seen from Fig. 3 [28]. The formation of the Cr-Cr dumbbell was never observed in alloys with C_{Cr} up to 10%. Very rarely, the formation of Cr-Cr dumbbells was seen in Fe-15%Cr [27].

The results of MD simulations suggested the presence of some deep traps for an SIA, whose concentration seemed to increase with Cr content [27]. As has been already mentioned the Cr-SIA interaction depends significantly on the local atomic environment, so that in concentrated alloys the free energy of the formation of an SIA constantly changes while the latter is migrating in the lattice. Static calculations were performed to provide the characterization of possible traps for SIAs in the concentrated alloys [27].

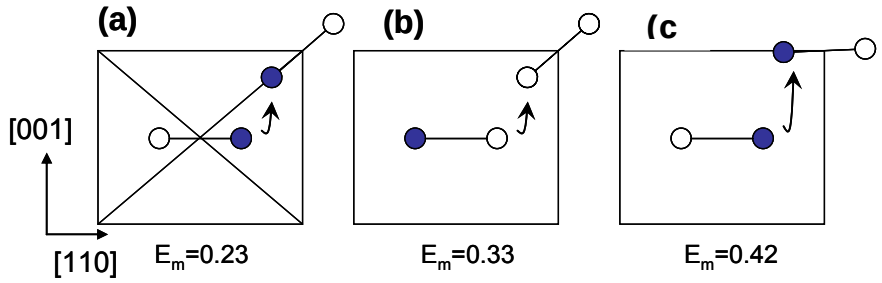

Fig. 3. Migration energy and path of the mixed [110] Fe-Cr dumbbell into: (a) [101] Fe-Cr dumbbell, (b) [101] Fe-Fe dumbbell and (c) [110] Fe-Cr dumbbell, as obtained by DFT calculations [28]. A filled circle denotes a Cr atom

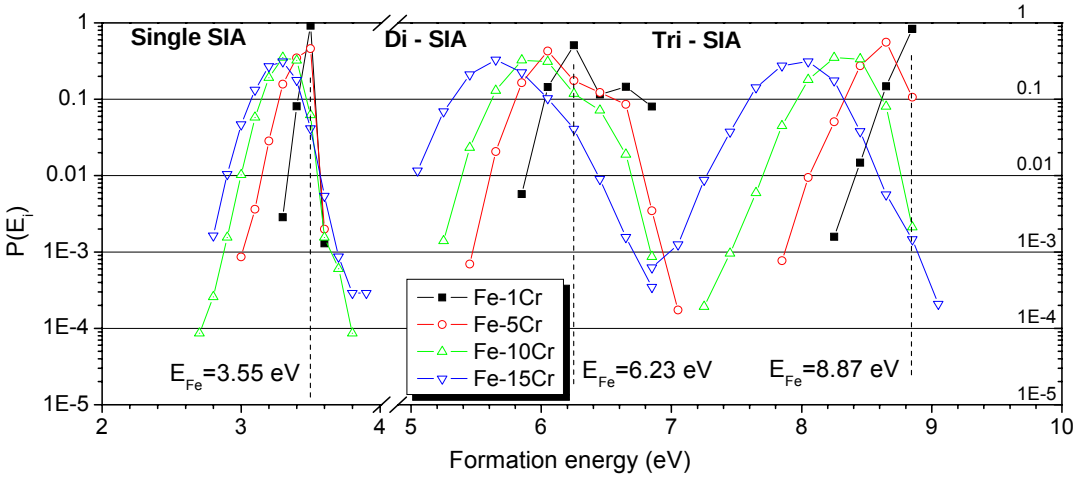

Fig. 4. Distribution of the formation energy of single SIA, di- and tri-SIA clusters in Fe-Cr alloys of different content, estimated by static calculations with the 2BM potential in [29]

The distribution of the formation energy probability, $P(E_f)$, was calculated for the random alloys with C_{Cr}=1-15%. $P(E_f)$ for single SIA, di-SIA and tri-SIA in Fe-Cr alloys is plotted in Fig. 4 [29]. The formation energies of the same defects, in their lowest energy configurations in pure Fe, are shown as vertical lines in the figure. With increasing Cr content $P(E_f)$ broadens showing the presence of the low-energy states with probability ~10^{-3} and lower. Based on this data, the strength and concentration of the strongest traps was estimated for the SIA defects in the alloys, as proposed in [27] and summarized in Tabl. 1. The latter shows that the trapping energy varies from 0.2 to 0.8 eV, depending on a defect size, generally increasing with C_{Cr}.

Table 1

Trap concentrations (atomic fraction) and energies (eV) for 3d-migrating sia defects in Fe-Cr alloys [29]

Defect	Quantity	Fe-1%Cr	Fe-5%Cr	Fe-10%Cr	Fe-15%Cr
Single SIA	C_{trap}	$2.8\cdot10^{-3}$	$8.6\cdot10^{-4}$	$8.6\cdot10^{-5}$	$1.6\cdot10^{-3}$
	E_{trap}	0.2	0.3	0.5	0.3
Di-SIA	C_{trap}	$5.7\cdot10^{-3}$	$6.9\cdot10^{-4}$	$1.3\cdot10^{-3}$	$1.1\cdot10^{-2}$
	E_{trap}	0.2	0.4	0.4	0.4
Tri-SIA	C_{trap}	$1.5\cdot10^{-3}$	$7.7\cdot10^{-4}$	$1.9\cdot10^{-4}$	$6.25\cdot10^{-4}$
	E_{trap}	0.4	0.6	0.8	0.8

3.4. Effect of Cr on the diffusivity of 1D-migrating SIA defects

The strong crowdion-Cr binding energy, found by DFT and confirmed by calculations using the 2BM potential [27], transfers to the SIA clusters as well. Crowdions in <111> SIA clusters exhibit binding energy which varies from 0.4 to 0.15 eV depending on the position of a crowdion in the cluster habit plane and the size of a cluster. The strongest interaction occurs at the cluster edge and the weakest in the center. The Cr-SIA cluster binding energy, estimated for crowdions at the edge of a cluster, decreases with cluster size down to ~0.15 eV, which is close to the binding energy of the Cr and the perfect edge dislocation.

MD studies of the mobility of <111> SIA clusters were performed in random Fe-Cr alloys with different Cr content using the 2BM potential [30]. A significant reduction in the diffusivity of <111> SIA clusters was observed in Fe-Cr alloys as compared to pure Fe. The actual value of the diffusivity reduction depends on three parameters: temperature, cluster size and Cr content. The most convenient way to represent obtained MD results is to give the ratio between the diffusion coefficients in Fe-Cr and in Fe ($R_n=D_n^{Fe\text{-}Cr}/D_n^{Fe}$, where n is the size of the cluster). The Cr concentration dependence of R_n, estimated at 350 °C, is shown in Fig 5,a. The left-hand axis of Fig. 5,a shows the change in the SIA cluster free energy, ΔF^{MD}, as defined in [31] as:

$$\Delta F_n^{MD} = k_B T \ln(D_n^{FeCr} / D_n^{Fe}) \quad (1)$$

The reduction of the diffusivity is strong and non-linear: R_7 reaches a minimum 10^{-2} at 10% Cr, meaning that the diffusion coefficient is a hundred times smaller in Fe-10%Cr than in pure Fe. With increasing the cluster size, the minimum diffusivity shifts towards smaller Cr concentration and R_n increases, e.g. R_{91}=0.1 at 2%Cr.

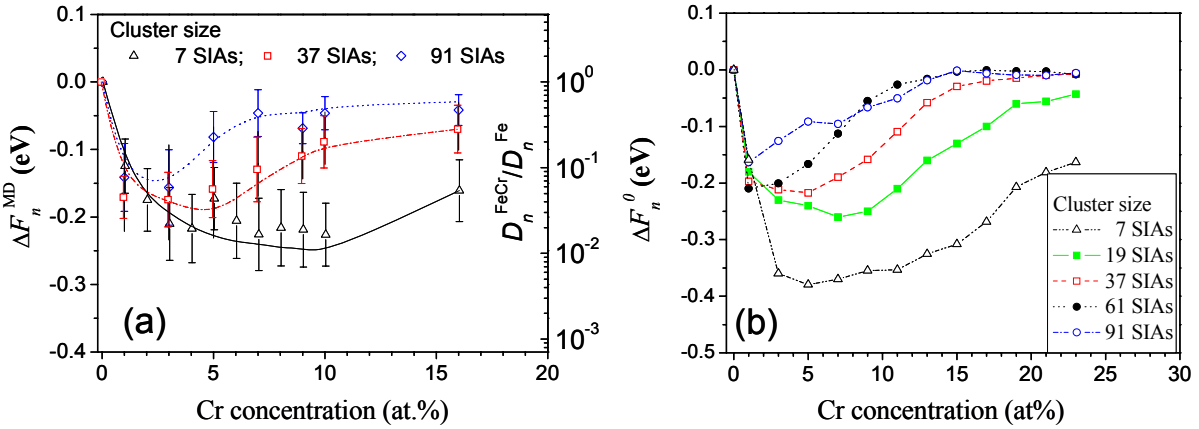

Fig. 5. Reduction in the diffusion coefficient and variation of the free energy of <111> SIA clusters in Fe-Cr alloys (at T=350 °C) as compared to pure Fe, estimated using (a) MD and (b) static calculations [30]

In order to rationalise obtained MD results the physical process of SIA cluster migration in Fe-Cr was modelled by expressing the reduction of the diffusion coefficient, R_n, in terms of the average binding energy E_b seen by the cluster due to the presence of Cr for a given solute concentration [31]. The model implies that the cluster moves in a field of energy hills and valleys, determined by the changing local atomic environment. The decrease of the cluster diffusivity comes from the increase of the time the cluster spends in the different positions, as compared with the pure crystal, which is proportional to $\exp(E_b / k_B T)$, where k_B is Boltzmann's constant and T is the absolute temperature. The diffusion coefficient of the cluster in Fe-Cr, $D^{Fe\text{-}Cr}$, then could be expressed knowing the corresponding in pure Fe, D^{Fe}, as:

$$D_n^{FeCr} = D_n^{Fe} \langle e^{E_b / k_B T} \rangle^{-1} = D_n^{Fe} e^{\Delta F / k_B T}, \quad (2)$$

where the averaging is performed over different cluster positions in the system. ΔF defined in Eqs. (1) and (2) and estimated using static simulations is presented in Fig. 5, b. It has been therefore shown that the model developed in [31] clearly succeeds in capturing the basic cause for SIA cluster slowing down in Fe-Cr alloys, compared to pure Fe, not only qualitatively, but also quantitatively. These results are however, only valid for the random alloys. It can be seen from Fig. 5, b that the saturation of the Cr-crowdion interaction occurs for C_{Cr}>12%. In this range of concentrations the α-α' phase separation may occur.

3.5. Interaction of SIA defects with Cr precipitates

Fe-Cr alloys as well as high-Cr ferritic steels containing more 10% Cr exhibit α-α' phase separation, which results in the formation of finely dispersed Cr-rich precipitates. These are coherent with the matrix and contain about 95% Cr. Experimental measurements show that the precipitates may exhibit extremely high density (up to 10^{24} m^{-3}) [8] at the onset of the phase separation and therefore may play an important role in the microstructure evolution if they somehow affect mobility of radiation defects.

Table 2

Formation energies (eV) of sia defects in pure chromium for ⟨110⟩ and ⟨111⟩ configurations. Data for pure fe is given in brackets [20]

Method	EIP calculations [29]		*Ab initio* calculations [28]	
Defect	⟨110⟩ config.	⟨111⟩ config.	⟨110⟩ config.	⟨111⟩ config.
E_f (SIA)	5.59 (3.59)	5.62 (4.01)	5.68 (3.75)	5.76 (4.45)
E_f (di-SIA)	10.31 (6.23)	9.55 (6.68)	10.24 (6.68)	10.11 (7.43)
E_f (tri-SIA)	14.78 (8.87)	13.91 (9.46)	14.72 (9.49)	14.08 (10.01)
E_f (vacancy)	2.56 (1.71)		2.71(2.15*) [23]	

The interaction of SIA defects with Cr-rich coherent precipitates was recently studied in [29]. Where the corresponding formation energies of a single SIA and di- and tri-SIAs in Fe-Cr, estimated using DFT and 2BM were reported and are summarized in Tabl. 2. Comparison of these results with the data presented in Fig. 2, reveals that the formation or migration of SIA-type defects in the Cr precipitates is strongly unfavourable, because of the large excess of the formation energy. The excess of the formation energy of a vacancy is about 0.5 eV. However, a vacancy was found to be slightly bound to the Cr precipitate (the latter is oversized), with the energy ~0.1 eV. This is, however, much less than the variation of the formation energy of a vacancy in the concentrated Fe-Cr alloys, estimated to vary from 0.2 to 0.4 eV in Fe-5%Cr and Fe-10%Cr, respectively. Based on these results, one expects that the Cr precipitates will act as 'scattering' centers for 3D-migrating SIA defects and not affect their mobility. Weak attractive vacancy-precipitate interaction will be effectively 'screened' due to the presence of dispersed Cr atoms in the depleted matrix around Cr precipitates. The formation and accumulation of both interstitials and vacancies inside the Cr precipitates is excluded.

The interaction of <111> SIA defects with the Cr precipitates in Fe10Cr matrix was studied using static and MD simulations in [30]. MS calculations revealed the presence of the strong repulsive interaction occurring when the <111> SIA cluster approaches the precipitate. The maximum repulsive energy was found when the <111> SIA cluster is located at the precipitate-matrix interface. The origin of the observed strong repulsion is the large formation energy excess of <111> SIAs, as has been already discussed in the previous section. By increasing the precipitate size, the energy barrier increases as well. The typical values of the repulsive energy of <111> SIA clusters (with sized varied from 7 to 331

defects) reported in [30] for precipitates with size of 1.5-3 nm, vary from 5 up 30 eV. Such energy barriers are not expected be surmounted with the help of thermal fluctuations. Thus large 1D migrating clusters are expected to be pinned (or immobilized) between Cr precipitates.

4. MOBILITY OF RADIATION INDUCED SELF-INTERSTITIAL DEFECTS IN Fe-Cr ALLOYS: SUMMARY

Gathering results and discussion presented in sections 3.3; 3.4 and 3.5, we provide a brief summary of the most important effects of Cr on the mobility of SIA defects and their clusters in dilute and concentrated Fe-Cr alloys.

3D-migrating (i.e. single SIAs and small SIA clusters containing up to defects):

- in dilute Fe-Cr alloys, can be trapped by single Cr and pairs of Cr atoms, with binding energies not exceeding 0.2 eV. In addition, the migration energy of the mixed Fe-Cr dumbbell is about 0.1 eV lower than that of the <110> Fe-Fe dumbbell;
- in concentrated Fe-Cr alloys, may encounter configurational traps involving a few Cr atoms, with binding energies in the range of about 0.2-0.8 eV. The concentration and the strength of these traps strongly depend on the Cr content;
- are not bound to the Cr precipitates and are not expected to accumulate inside them. The Cr precipitates therefore do not affect mobility of these defects.

1D-migrating interstitial clusters:

- with increasing Cr concentration, their diffusivity first decreases and then increases again. The diffusivity reduction exhibits a minimum at a certain Cr content. The depth and critical concentration at which the minimum occurs depends on the cluster size.
- with size of about 7-30 SIAs exhibit the minimum diffusivity at 6-10% Cr;
- with increasing cluster size, the minimum diffusivity shifts towards lower concentrations and stays at ~1 %Cr for small dislocation loops (i.e. 2-3 nm);
- are not bound to Cr precipitates and are not expected to penetrate inside them. The Cr precipitates therefore cause an effective pinning of these clusters and hence dramatically reduce their mobility.

5. IMPLICATIONS OF THE RESULTS PROVIDED BY ATOMISTIC SIMULATIONS AND CONCLUSIONS

As shown, in Fe-Cr alloys the microstructure evolution under irradiation is the consequence of strongly coupled, concomitant phase changes and defect migration processes that inextricably influence each other. The strong reduction of the mobility of <111> SIA clusters and small dislocation loops (in Fe-Cr as compared to Fe) should lead to a pronounced decrease of annihilation of small 1D-migrating SIA clusters, created in collision cascades initiated by fast neutrons, at dislocations, grain boundaries and other sinks. Meaning that additional recombination sites for freely migrating vacancies and small vacancy clusters will be provided. This should lead to a lower equilibrium vacancy concentration and a decrease in swelling. In addition, the nucleation rate of the dislocation loops is expected to be higher in Fe-Cr alloys, but their growth rate correspondingly lower, because of the reduced mobility of 3D-migrating SIAs (coupled with the unaffected vacancy migration). This agrees well with the experimental results from [10], mentioned already in Section 2.

The decrease of <111> SIA cluster diffusivity is non-monotonic in the random solution limit. Small clusters with size up to 20 SIAs exhibit a diffusivity minimum at 9-12% Cr, which shifts towards lower Cr concentrations with the cluster size, as schematically shown in Fig. 6,a. At elevated temperatures and/or under irradiation either Cr ordering or α-α' phase separation is expected to occur, depending on the Cr content in the alloy. Strong repulsive interaction between Cr precipitates and <111> SIA clusters will result in further suppression of the mobility of these defects. The cross section of the <111> SIA cluster - precipitate interaction depends on the density of precipitates and size of a cluster and precipitate. The onset of the α-α'-phase separation results in the formation of nanometric Cr precipitates with enormously

high density (up to 10^{24} m^{-3}) [8]. Coalescence of Cr precipitates with the corresponding decrease of the precipitate density should 'soften' the blockage of 1D-migrating clusters by α' particles.

In the low-concentration alloys, the enhanced Cr ordering should lead to a strong decrease of the value of ΔF (defined in Section 3.4). The mobility of <111> SIA clusters will be governed by the interaction with isolated Cr atoms and therefore the migration energy should have a weak dependence on the cluster size and will stay around 0.4-0.3 eV for the small (in-cascade created) SIA clusters. The degree of ordering, in turn, depends on the heat of mixing and temperature, thus the alloys containing around 5% Cr should have the lowest SRO parameter. The change in the diffusivity reduction due to the effect of Cr ordering/precipitation is schematically shown in Fig. 6,b.

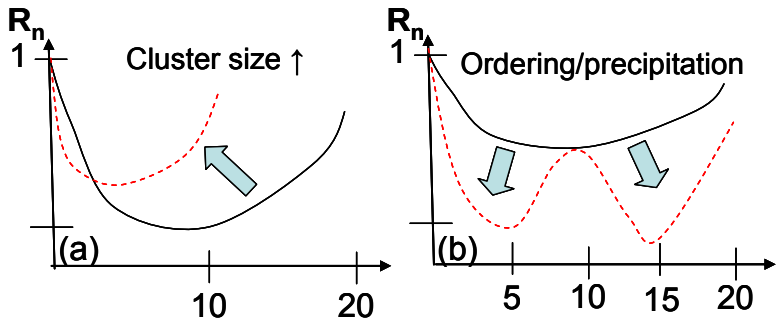

Fig. 6. Variation of the diffusivity reduction ($Rn=D^{Fe-Cr}/D^{Fe}$) of 1D-migrating SIA clusters (a) due to the increase of a cluster size and (b) in the presence of the long-range order or Cr precipitation. Dashed curves show the trend

The pinning of <111> SIA clusters by α' particles should lead to a steep increase of the nucleation rate of ½<111> loops. The formation of <100> loops was proposed to occur via unfaulting of small ½<111> loops [33] or in the reaction between the two ½<111> loops [34]. So far, there is no experimental confirmation for the proposed mechanisms. If, however, these mechanisms are relevant, the nucleation rate and the density of <100> loops should increase in the presence of α-α' phase separation. The experimental data shown in Fig.1,c, reveals a steep increase in the density of <100> loops in alloys with C_{Cr}=12-18%Cr, irradiated at 425 °C, which potentially should exhibit α-α'-phase separation [32].

By combining these observations, the general picture of void swelling behaviour as a function of Cr content can be built. The swelling minimum experimentally observed at relatively low doses (1-10 dpa) around 10% Cr (see Fig. 1,a) can be mainly attributed to the reduction of the mobility of in-cascade created <111> SIA clusters. Consequently, the minimum of the hardening also stays around 9-10% Cr (see Fig.1,a), since the mean size of defects (mainly of SIA type) obstructing the motion of dislocations is minimal in these alloys. With increasing dose (and irradiation temperature) the α' precipitation or Cr ordering occurs, in the alloys with C_{Cr}=10-20% (spinodal decomposition occurs at larger C_{Cr}) and around 5%, respectively. As a consequence of these effects, <111> SIA clusters will be more effectively reduced either in high-Cr or low-Cr alloys, providing a local maximum at ~10% Cr. Indeed, the swelling, measured at higher temperature or dose usually shows two separated minima (see Fig. 1,a). In the temperature range where Cr ordering/precipitation is no longer possible the swelling minimum is restored at ~10% Cr.

Concluding, we provided evidence from atomistic modelling that the reduction of ½<111> dislocation loops and small 3D-migrating SIA clusters, the formation of <100> loops, induced swelling and hardening are interconnected, and all strongly depend on the Cr content. Two main characteristics of the Fe-Cr system seem to provide in many cases the key for the interpretation of the behaviour of these alloys under irradiation as observed experimentally. These characteristics are: (i) the change of sign of the mixing enthalpy from negative to positive in the low Cr concentration region; (ii) the existence of a strong interaction between self-interstitials and Cr atoms, which dramatically reduces the diffusivity of 1D-migrating self-interstitial atom clusters in Fe-Cr compared to Fe.

REFERENCES

1. R. Klueh, D. Harries. High-Chromium Ferritic and Martensitic Steels Nuclear Applications // *Astm Intl*. 2001.

2. D.S. Gelles // *J. Nucl. Mater*. 1995, v. 225 ; E.A. Little and D.A. Stow // *J. Nucl. Mater*. 1979, v. 87, p. 25; E.A. Little and D.A. Stow // *J. Metal Sci*. 1980, v. 14, p. 89.

3. D.S. Gelles // *J. Nucl. Mater*. 1995,v. 225, p. 163-174.

4. S.I. Porollo, A.M. Dvoriashin, A.N. Vorobyev, Yu.V. Konobeev // *J. Nucl. Mater.* 1998, v. 256, p. 247-253.

5. Y. Katoh, A. Kohyama, and D.S. Gelles // *J. Nucl. Mater*. 1995, v. 225, p. 154-162.

6. H. Kayano, A. Kimura, M. Narui, Y. Sasaki, Y. Suzuki, S. Ohta // *J. Nucl. Mater.* 1988, v. 155-157, p. 978; A. Kohyama, A. Hishinuma, D.S. Gelles, R.L. Klueh, W. Dietz, K. Ehrlich // *J. Nucl. Mater.* 1996, v. 233-237, p. 138.

7. M. Matijasevic, A. Almazouzi. Structural and Refractory Materials for Fusion and Fission Technologies // *MRS Proceedings.* 2006, v. 981E, p. 0981-JJ07-06.

8. P. Dubuisson, D. Gilbon, J.L. Séran // *J. Nucl. Mater*. 1993, v. 205, p. 178; M.H. Mathon, Y. de Carlan, G. Geoffroy, X. Averty, A. Alamo and C.H. de Novion // *J. Nucl. Mater.* 2003, v. 312, p. 236.

9. A. Okada, N. Kawaguchi, M.L. Hamilton, K. Hamada, T. Yoshiie, I. Ishida, E. Hirota // *J. Nucl. Mater*. 1994б v. 212-215, p. 382.

10. N. Yoshida, A. Yamaguchi, T. Muroga, Y. Miyamoto and K. Kitajima // *J. Nucl. Mater*. 1988, v. 155-157, p. 1232.

11. K. Arakawa, M. Hatanaka, H. Mori, K. Ono // *J. Nucl. Mater*. 2004, v. 329-333, p. 1194.

12. Yu.V. Konobeev, A.M. Dvoriashin, S.I. Porollo, F.A. Garner // *J. Nucl. Mater.* 2006, v. 355, p. 124.

13. I. Mirebeau, M. Hennion, G. Parette // *Phys. Rev. Lett.* 1984, v. 53, p. 687; N.P. Filippova, V.A. Shabashov, A.L. Nikolaev // *Phys. Met. & Metall*. 2000, v. 90, p. 145.

14. P. Olsson, I.A. Abrikosov, and J. Wallenius // *Phys. Rev. B*. 2006, v. 73, p. 104416.

15. T.P.C. Klaver, R. Drautz, and M.W. Finnis // *Phys. Rev. B*. 2006, v. 74, p. 094435.

16. M.Y. Lavrentiev, R. Drautz, D. Nguyen-Manh, T.P.C. Klaver, and S.L. Dudarev // *Phys. Rev. B*. 2007, v. 75, p. 14208.

17. P. Erhart, B. Sadigh and A. Caro // *Appl. Phys. Lett.* 2008, v. 92, p. 141904.

18. P. Olsson, J. Wallenius, C. Domain, K. Nordlund, and L. Malerba // *Phys. Rev. B*. 2005, v. 72, p. 214119.

19. G.J. Ackland, M.I. Mendelev, D.J. Srolovitz, S. Han and A.V. Barashev // *J. Phys: Condens. Matter*. 2004, v. 16, p. 1.

20. F. Willaime, C.C. Fu, M.C. Marinica, J. Dalla Torre // *Nucl. Instr. Meth. Phys. Res. B*. 2005, v. 228, p. 92-99.

21. K. Vörtler, C. Björkas, D. Terentyev, L. Malerba, K. Nordlund // *J. Nucl. Instr. Meth. Phys. Res. B*. 2008.

22. A.L. Nikolaev // *Phil. Mag.* 2007, v. 87, p. 4847.

23. P. Olsson, C. Domain, and J. Wallenius // *Phys. Rev. B.* 2007, v. 75, p. 014110.

24. D. Terentyev and L. Malerba // *J. Nucl. Mater.* 2004, v. 329-333, p. 1161.

25. D.A. Terentyev, L. Malerba, M. Hou // *Phys. Rev. B*. 2007, v. 75, p. 104108.

26. Yu.N. Osetsky, D. J. Bacon, A. Serra, B. N. Singh, and S. I. Golubov // *Phil. Mag.* 2003, v. 83, p. 61.

27. D. Terentyev, P. Olsson, T.C.P. Klaver, L. Malerba doi: 10.1016/j.commatsci. 2008.03.013.

28. P. Olsson. Ab initio study of interstitial migration in Fe-Cr alloys // *J. Nucl. Mater*. 2008.

29. D. Terentyev, P. Olsson, and L. Malerba. Diffusion of 3D-migrating self-interstitial clusters in dilute and concentrated Fe-Cr alloys // *J. Nucl. Mater*. 2008.

30. D. Terentyev, P. Olsson, L. Malerba, and A.V. Barashev // *J. Nucl. Mater*. 2007, v. 362, p. 167.

31. D.A. Terentyev, L. Malerba, and A.V. Barashev // *Phil. Mag. Lett*. 2005, v. 85, p. 587.

32. N. Saunders and A.P. Miodownik, CALPHAD calculation of Phase Diagrams, A comprehensive Guide // *Pergamon*. 1998, p.463.

33. B.L. Eyre and R. Bullough // *Philos. Mag*. 1965, v. 12, p. 31.
34. J. Marian, B.D. Wirth, A. Caro, B. Sadigh, G.R. Odette, J. M. Perlado, and T. Diaz de la Rubia // *Phys. Rev. B*. 2002, v. 65, p. 144102.
35. P. Olsson, I.A. Abrikosov, and J. Wallenius // *Phys. Rev. B*. 2006, v. 73, p. 104416.

НЕКОТОРЫЕ СТОРОНЫ ЭФФЕКТОВ РАДИАЦИОННЫХ ПОВРЕЖДЕНИЙ В СПЛАВАХ Fe-Cr С ТОЧКИ ЗРЕНИЯ АТОМИСТИЧЕСКОГО МОДЕЛИРОВАНИЯ

Д. Терентьев, П. Олсон

Сплавы Fe-Cr составляют основу ферритных сталей с высоким содержанием Cr, являющихся кандидатами в конструкционные материалы для атомных электростанций ближайшего будущего. В последнее время значительные усилия направлены на разработку теоретических моделей, рассматривающих реакцию сплавов Fe-Cr на облучение. В настоящей работе дается краткий обзор современного уровня понимания радиационных повреждений в сплавах Fe-Cr, при этом в основу берутся последние на данный момент результаты. В частности, дается обзор и подводится итог данных, полученных с помощью различных методов атомистического моделирования с целью определения наиболее важных результатов, достигнутых за последние несколько лет.

ДЕЯКІ СТОРОНИ ЕФЕКТІВ РАДІАЦІЙНИХ ПОШКОДЖЕНЬ У СПЛАВАХ Fe-Cr З ТОЧКИ ЗОРУ АТОМІСТИЧНОГО МОДЕЛЮВАННЯ

Д. Терентьєв, П. Олсон

Сплави Fe-Cr становлять основу феритних сталей с високим вмістом Cr, що являються кандидатами у конструкційні матеріали для атомних електростанцій найближчого майбутнього. В останній час значні зусилля спрямовані на розробку теоретичних моделей, які розглядають реакцію Fe-Cr-сплавів на опромінення. В даній роботі наводиться короткий огляд сучасного рівня розуміння радіаційних пошкоджень у сплавах Fe-Cr, при цьому за основу беруться останні на даний момент результати. Зокрема, наводиться огляд та підводиться підсумок даних, що отримані за допомогою різних методів атомістичного моделювання з метою визначення найбільш важливих результатів, які досягнуті за останні кілька років.